Research in Astron. Astrophys. **2011** Vol. **11** No. **2**, 205–224
http://www.raa-journal.org *http://www.iop.org/journals/raa*

Research in Astronomy and Astrophysics

Dynamics and control of a solar collector system for near Earth object deflection *

Shen-Ping Gong, Jun-Feng Li and Yun-Feng Gao

School of Aerospace, Tsinghua University, Beijing 100084, China; *gongsp@tsinghua.edu.cn*

Received 2010 July 1; accepted 2010 September 1

Abstract A solar collector system is a possible method using solar energy to deflect Earth-threatening near-Earth objects. We investigate the dynamics and control of a solar collector system including a main collector (MC) and secondary collector (SC). The MC is used to collect the sunlight to its focal point, where the SC is placed and directs the collected light to an asteroid. Both the relative position and attitude of the two collectors should be accurately controlled to achieve the desired optical path. First, the dynamical equation of the relative motion of the two collectors in the vicinity of the asteroid is modeled. Secondly, the nonlinear sliding-mode method is employed to design a control law to achieve the desired configuration of the two collectors. Finally, the deflection capability of this solar collector system is compared with those of the gravitational tractor and solar sail gravitational tractor. The results show that the solar collector is much more efficient with respect to deflection capability.

Key words: minor planets, asteroids — techniques: miscellaneous — solar collector

1 INTRODUCTION

Several authors have investigated the use of large solar reflectors to change the climate of a planet. Some explored the use of large solar reflectors above Mars to increase its planetary insolation as part of a large-scale terraforming effort (Oberg 1981; Birch 1992; Zubrin & McKay 1997; Fogg 1995; Maunter et al. 1990; McInnes 2002). Still others proposed large solar sail shields located near the interior Sun-Earth Lagrange point to reduce the solar flux incident on the Earth (Seifritz 1989; Early 1989; Hudson 1991; McInnes 2002). Melosh (1993) proposed using a large solar collector to deflect an asteroid. The solar collector is used to focus sunlight onto the surface of the asteroid to generate thrust as the surface's layers vaporize. However, the method was criticized for its impracticality and was rarely referred to since it was proposed. According to the formula given in (Melosh 1993), a 0.5 km solar sail collector operating for a year can deflect an asteroid up to 2.2 km in diameter, which is very effective compared with other strategies. Matloff (2008) checked the performance of this system. Kahle et al. (2006) investigated the overall physical limits of the collector and found that the bottleneck of the method is that the lifetime of the collector was very short because of the plume's influence from vaporized mass flow. To prolong the lifetime of the collector, two methods are proposed in (Melosh et al. 2002). The first one is a Cassegrain-like arrangement of two collectors: the main collector (MC) is placed far from the asteroid to avoid the mass flow and a secondary collector

* Supported by the National Natural Science Foundation of China.

(SC), which is much smaller in diameter, is placed at the focal point of the MC. The SC will receive the sunlight collected by the MC and direct it to the asteroid's surface. The SC will be steered away from the asteroid after the end of its lifetime if a multi-SC system is proposed. The second method is to transmit the energy not simply by collection of natural sunlight, but by first converting the sunlight into a small-divergence laser or microwave beam. Such a system can be placed at a large distance from the asteroid because of the small-divergence of the laser beam. However, the technical complexity of the second method makes it more impractical than the first method. The first method has a high-accuracy requirement on the position and attitude of the two collectors. To design a high-accuracy control mechanism, the positions and attitudes of the two collectors are considered as a system in this paper. The control accuracy and the propellant requirement for maneuvering the two collectors are discussed. Finally, with all the physical limitations considered, the deflection capability of the system is evaluated again and compared with those of the gravitational tractor and solar sail gravitational tractor.

2 THE LIFETIME EVALUATION AND FOCAL LENGTH SELECTION

The dependency of mass flow on the energy flux is illustrated in Figure 1 and the vaporized mass flow increases with energy flux at the spot. The calculation process is given in Appendix A. To generate large reaction thrusts, it is more efficient to increase the intensity than to increase the illumination area because the mass flow increases with the energy flux quadratically. The energy intensity can be intensified by increasing the radius of the collector or decreasing the focal length of the collector. Increasing the radius of the collector is restricted by physical limitations. Decreasing the focal length will reduce the illumination area at the spot and seems attractive. However, a short focal length requires the collector to be close to the asteroid, which will greatly decrease the lifetime of the collector. A collector with a 315-m radius is used for this analysis and the lifetime of the collector is evaluated when the focal length is varied, as shown in Figure 2. The figure illustrates that the lifetime will only be several seconds if the focal length is within 900 m and it can be greatly prolonged if the focal length increases because the expected lifetime increases approximately exponentially with focal length. The lifetime can be several years if the MC can be placed several kilometers away from the asteroid (the focal length is several kilometers).

Prolonging the lifetime requires increasing the focal length and increasing the energy intensity at the spot requires decreasing the focal length. Therefore, prolonging the lifetime counterbalances increasing the energy intensity, as shown in Figure 2. The reaction force generated by the mass flow decreases with the focal length and the lifetime increases with it. The total impulse exerted on the asteroid increases with the focal length when the focal length is less than a critical value and

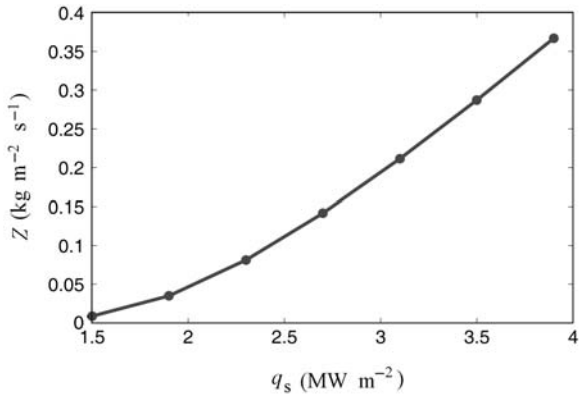

Fig. 1 Mass flow of the different energy fluxes.

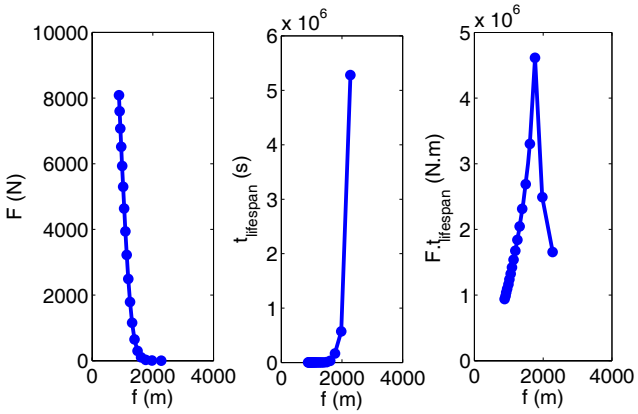

Fig. 2 Dependencies of the reaction force and lifetime on the focal length.

reaches the maximum at that value. Therefore, the optimal focal length can be chosen to maximize the velocity variation of the asteroid. This property also implies that the maximal range in variation of velocity of the collector cannot be improved upon by adjusting the focal length.

In a word, the bottleneck of this method is the short lifetime of the collector because of the plume impingement. One of the two approaches proposed to prolong the lifetime of the collector is to implement a Cassegrain-like arrangement with two collectors. The MC is placed far away from the asteroid and only the SC is exposed to the hot gas and ejected dust. The relative attitude of the MC and SC are properly designed to guarantee that the solar light collected by the MC will reach the secondary one and then be directed to the asteroid. The diameter of the SC should be larger than the spot diameter to guarantee that the collected solar light will be fully redirected. Large focal length of the MC requires a large-diameter SC. The energy transferred to the asteroid by the SC is the same as that collected by the MC. Therefore, the lifetime of the SC is the same as that of a single collector of the same size as the MC.

Since the Sun is not a point source, the spot of sunlight condensed by the collector is dependent on the focal length of the collector. Furthermore, the Cassegrain-like arrangement will enlarge the spot's diameter on the asteroid, which reduces the resulting energy density on the asteroid's surface. Considering the collector's reflectivity, the finite size (non-point) of the Sun, the near Earth asteroids' (NEA's) surface absorption coefficient, and out-of-line collector arrangement, a total energy transfer efficiency of the system less than one can be assumed, with the exact value being dependent on the geometrical parameters of the arrangement, the optical parameters of the collectors and the asteroid's surface material. Detailed discussions of the two collectors' design and the efficiency calculations can be found in Kahle et al. (2006) and Melosh et al. (2002), respectively. This paper focuses on the dynamics and control of the system.

3 DYNAMICAL EQUATIONS OF THE SYSTEM

A configuration shown in Figure 3 is discussed in this paper, where the MC is placed several kilometers away from the asteroid and the aperture faces the Sun to collect sunlight. The SC is placed right behind the asteroid and redirects the collected sunlight to the asteroid's surface. The position and attitude of both collectors are accurately controlled to redirect the light after the two-level convergence to the asteroid's surface. The position of the MC is designed to be at a position above the asteroid. The SC is placed at the focal point of the MC and the distance between the SC and the asteroid is equal to the focal length of the SC. The attitude of the SC is determined by the relative positions of the three objects. Either position or attitude error of the MC will lead to an increase in the spot's

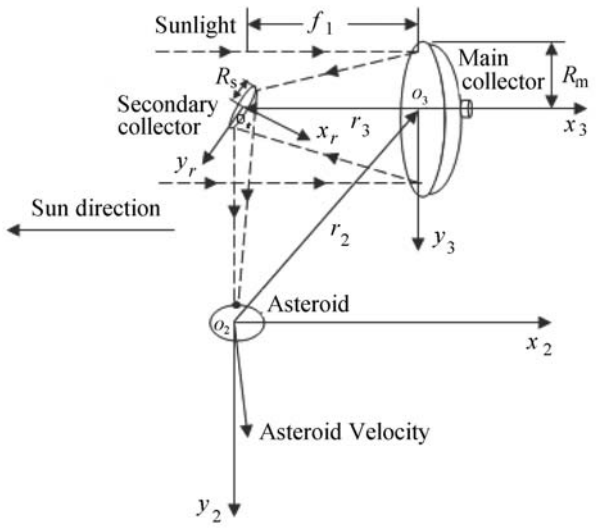

Fig. 3 A Cassegrain-like arrangement of the collector system.

diameter on the asteroid and a decrease in the energy flux, which leads to a decrease in mass flow. Therefore, accurate position and attitude of the MC are preconditions to the success of the system. Under this precondition, the position and attitude accuracy of the SC will determine the amount of sunlight received and energy flux at the spot on the asteroid. In short, any error in the position or attitude will degrade the deflection capability of the system. Therefore, the control accuracy of the system should be investigated to analyze the feasibility of the system. The dynamical and control analysis are based on the following assumptions:

(1) The asteroid is in a Keplerian elliptical orbit around the Sun;
(2) The extra forces exerted on the sail include the gravitational forces of the Sun and the asteroid, the solar radiation pressure force, and an unknown but bounded perturbation force;
(3) The extra torques exerted on the sail include the gravitational torques of the Sun and asteroid, the solar radiation pressure torque, and an unknown but bounded perturbation torque.

To analyze the dynamics and control of the collectors, three reference frames are defined.

- $o_2x_2y_2z_2$: the origin is the center of mass of the asteroid; the x_2 axis points from the Sun to the asteroid; the z_2 axis is defined by the angular momentum of the asteroid; the y_2 axis forms a right-handed triad with the x_2 and z_2 axes.
- $o_3x_3y_3z_3$ (body-fixed frame of the MC): the origin is the mass center of the MC; the x_3 axis is along the central axis of the collector; the y_3 and z_3 axes are in the plane perpendicular to the central axis and fixed on the collector.
- $o_{\mathrm{r}}x_{\mathrm{r}}y_{\mathrm{r}}z_{\mathrm{r}}$ (body-fixed frame of the SC): the origin is the center of mass of the reflector; the x_{r} axis is along the normal of the reflector; the y_{r} and z_{r} axes are in the reflector plane and fixed on the reflector.

The MC is desired to be in a static equilibrium in the frame $o_2x_2y_2z_2$ and the equilibrium is uniquely determined by focal lengths of the two collectors. When small position errors of the MC exist, the SC is controlled to track the focal point of the MC. The attitude of the MC will track the reference attitude generated by arranging its aperture to face the sunlight. The optical characteristic of the SC should be designed to redirect the reflected light from the MC to reach the

asteroid's surface. The reference attitude information depends on the optical characteristic of the SC and different optical characteristics will generate different reference information. In this paper, the normal to the SC is regarded as the bisection of the angle formed by the incident and reflected light. The collectors are controlled in the vicinity of the asteroid and the aperture of the MC is expected to face the Sun so that the parallel solar light can be focused. The dynamics of the MC in the vicinity of the asteroid can be written in the following form:

$$\ddot{\boldsymbol{r}}_2 + 2\boldsymbol{\omega}_2{}^{\mathrm{o}} \times \dot{\boldsymbol{r}}_2 + \boldsymbol{\omega}_2{}^{\mathrm{o}} \times (\boldsymbol{\omega}_2{}^{\mathrm{o}} \times \boldsymbol{r}_2) + \dot{\boldsymbol{\omega}}_2{}^{\mathrm{o}} \times \boldsymbol{r}_2 = \boldsymbol{f}_2{}^{\mathrm{s}} + \boldsymbol{f}_2{}^{\mathrm{a}} + \boldsymbol{f}_2{}^{\mathrm{solar}} + \boldsymbol{f}_2{}^{\mathrm{pert}}, \quad (1)$$

where $\boldsymbol{r}_2$ is position vector from the asteroid to the collector in $o_2x_2y_2z_2$, $\boldsymbol{\omega}_2{}^{\mathrm{o}}$ the angular velocity of the frame $o_2x_2y_2z_2$, and $\boldsymbol{f}_2{}^{\mathrm{s}}$, $\boldsymbol{f}_2{}^{\mathrm{a}}$, $\boldsymbol{f}_2{}^{\mathrm{solar}}$ and $\boldsymbol{f}_2{}^{\mathrm{pert}}$ denote the solar gravity acceleration exerted on the MC, the gravity acceleration of the asteroid exerted on the MC, the solar radiation acceleration exerted on the MC and the perturbation force exerted on the MC, respectively.

Different terms of the equation are given by

$$\begin{aligned}
\left|\boldsymbol{\omega}_2{}^{\mathrm{o}}\right| &= \dot{f}_{\mathrm{a}} = n_{\mathrm{a}} \frac{(1 + e_{\mathrm{a}} \cos f_{\mathrm{a}})^2}{(1 - e_{\mathrm{a}}^2)^{\frac{3}{2}}}, \\
\left|\dot{\boldsymbol{\omega}}_2{}^{\mathrm{o}}\right| &= \ddot{f}_{\mathrm{a}} = -\frac{2n_{\mathrm{a}}^2 (1 + e_{\mathrm{a}} \cos f_{\mathrm{a}})^3 e_{\mathrm{a}} \sin f_{\mathrm{a}}}{(1 - e_{\mathrm{a}}^2)^3}, \\
\boldsymbol{f}_2{}^{\mathrm{s}} &= \frac{\mu_{\mathrm{s}}}{|\boldsymbol{r}_1|^3} \boldsymbol{r}_1 - \frac{\mu_{\mathrm{s}}}{|\boldsymbol{r}_1 + \boldsymbol{r}_2|^3} (\boldsymbol{r}_1 + \boldsymbol{r}_2), \\
\boldsymbol{f}_2{}^{\mathrm{a}} &= -\frac{\mu_{\mathrm{a}}}{|\boldsymbol{r}_2|^3} \boldsymbol{r}_2,
\end{aligned}$$

where f_{a} is the true anomaly, e_{a} is the eccentricity of the asteroid orbit and n_{a} is the mean angular velocity of the asteroid rotating around the Sun; μ_{s} and μ_{a} denote gravitational constant of the Sun and the asteroid, respectively; $\boldsymbol{r}_1$ is position vector from the Sun to the asteroid in $o_2x_2y_2z_2$.

Also, $\boldsymbol{f}_2{}^{\mathrm{solar}}$ is determined by the attitude of the collector and can be given analytically according to its shape. In this paper, the collector is assumed to be the surface of a hemisphere and the surface integral is employed to calculate the solar radiation pressure force. The calculation of the solar radiation pressure force is (as shown in Appendix B) given by

$$\begin{aligned}
\boldsymbol{F}_{\mathrm{s}} &= m_2 \boldsymbol{f}_2{}^{\mathrm{solar}} = 2P \int_0^{\pi/2} \int_0^{2\pi} \left(\boldsymbol{n}_i \cdot \boldsymbol{n}_2{}^{\mathrm{s}}\right)^2 \boldsymbol{n}_i R^2 \sin\gamma d\gamma d\varphi \\
&- R_1(-\varphi_{\mathrm{s}}) R_3(\pi/2 - \gamma_{\mathrm{s}}) 3P \int_0^{\gamma_{\mathrm{s}}} \int_0^{2\pi} \left(\boldsymbol{n}_i \cdot \boldsymbol{n}_2{}^{\mathrm{s}}\right)^2 \boldsymbol{n}_i R^2 \sin\gamma d\gamma d\varphi, \quad (2)
\end{aligned}$$

where m_2 (m_3) is the mass of MC (SC), R_1 is position vector from the Sun to the asteroid in $o_2x_2y_2z_2$. Here $R_i(\theta)(i = 1, 2, 3)$ is transition matrix generated by Euler rotation, $\boldsymbol{n}_2(\boldsymbol{n}_3)$ the normal vector of the MC (SC), γ is a cone angle and φ a clock angle. Also, P is the solar radiation pressure at the distance of the asteroid.

The sunlight direction can be projected in the frame $o_3x_3y_3z_3$ as

$$\boldsymbol{n}_2{}^{\mathrm{s}} = \mathbf{A}_2 \frac{\boldsymbol{r}_1 + \boldsymbol{r}_2}{|\boldsymbol{r}_1 + \boldsymbol{r}_2|}, \quad (3)$$

where $\mathbf{A}_2$ is transition matrix frame $o_2x_2y_2z_2$ to $o_3x_3y_3z_3$.

The perturbation force ${\boldsymbol{f}_2}^{\mathrm{pert}}$ is assumed to be a bounded unknown perturbation force exerted on the collector, and the perturbation satisfies the following constraint

$$|{\boldsymbol{f}_2}^{\mathrm{pert}}| \leq f_2^{\mathrm{m}}. \tag{4}$$

The relative orientation of the MC with respect to the frame $o_2x_2y_2z_2$ is described by three Euler angles $(\varphi_2, \theta_2, \psi_2\ )$ of the rotational sequence of $R_3(\psi_2) \leftarrow R_2(\theta_2) \leftarrow R_1(\varphi_2)$ from the frame to the body-fixed frame $o_3x_3y_3z_3$. The angular velocity $({\boldsymbol{\omega}_2}^{\mathrm{b}})$ components of the collector in the frame $o_3x_3y_3z_3$ can be given by

$${\boldsymbol{\omega}_2}^{\mathrm{b}} = \begin{bmatrix} \dot{\varphi}_2 - \dot{\psi}_2 S_{\theta_2} \\ \dot{\theta}_2 C_{\varphi_2} + S_{\varphi_2} C_{\theta_2} \dot{\psi}_2 \\ -\dot{\theta}_2 S_{\varphi_2} + \dot{\psi}_2 C_{\varphi_2} C_{\theta_2} \end{bmatrix} + \mathbf{A}_2 \Big({\boldsymbol{\omega}_2}^{\mathrm{o}} + \frac{\boldsymbol{r}_2 \times \dot{\boldsymbol{r}}_2}{|\boldsymbol{r}_2|^2} \Big), \tag{5}$$

The kinematical differential equations can be solved from Equation (5), given by

$$\dot{\chi}_2 = \begin{bmatrix} \dot{\psi}_2 \\ \dot{\theta}_2 \\ \dot{\varphi}_2 \end{bmatrix} = \begin{bmatrix} \omega_2^y S_{\varphi_2}/C_{\theta_2} + \omega_2^z C_{\varphi_2}/C_{\theta_2} \\ \omega_2^y C_{\varphi_2} - \omega_2^z S_{\varphi_2} \\ -\omega_2^x + \omega_2^y S_{\varphi_2} S_{\theta_2}/C_{\theta_2} + \omega_2^z C_{\varphi_2} S_{\theta_2}/C_{\theta_2} \end{bmatrix} = \boldsymbol{G}_2(\omega_2), \tag{6}$$

where $\chi_2 = (\varphi_2\ \theta_2\ \psi_2)$ are three Euler angles of MC in frame $o_2x_2y_2z_2$, and

$$\boldsymbol{\omega}_2 = \begin{bmatrix} \omega_2^x & \omega_2^y & \omega_2^z \end{bmatrix}^{\mathrm{T}} = {\boldsymbol{\omega}_2}^{\mathrm{b}} - \mathbf{A}_2 \left({\boldsymbol{\omega}_2}^{\mathrm{o}} + \frac{\boldsymbol{r}_2 \times \dot{\boldsymbol{r}}_2}{|\boldsymbol{r}_2|^2} \right), \quad S_{\varphi_2} = \sin\varphi_2,$$

Three axes of the body-fixed frame are chosen to be the principle axes of inertia. Then, the inertia matrix is diagonal when described in the body-fixed frame. The solar radiation force will generate a torque when the pressure center is offset from the mass center. The gravitational torques of the Sun and the asteroid are not zero when the body-fixed frame is not consistent with the orbital frame. Other perturbation effects smaller than these torques are considered to be bounded perturbations in this paper. Therefore, the dynamical equation of the attitude in the frame $o_3x_3y_3z_3$ is written as

$$\mathbf{I}_2 \dot{\boldsymbol{\omega}}_2{}^{\mathrm{b}} + {\boldsymbol{\omega}_2}^{\mathrm{b}} \times \left(\mathbf{I}_2 \cdot {\boldsymbol{\omega}_2}^{\mathrm{b}} \right) = {\boldsymbol{M}_2}^{\mathrm{s}} + {\boldsymbol{M}_2}^{\mathrm{a}} + {\boldsymbol{M}_2}^{\mathrm{solar}} + {\boldsymbol{M}_2}^{\mathrm{c}} + {\boldsymbol{M}_2}^{\mathrm{pert}}, \tag{7}$$

where $\mathbf{I}_2(\mathbf{I}_3)$ is the inertia matrix of MC (SC), $\boldsymbol{M}_2^{\mathrm{s}}$ $(\boldsymbol{M}_3^{\mathrm{s}})$ is the gravity torque of the sun exerted on the MC (SC), $\boldsymbol{M}_2^{\mathrm{a}}$ $(\boldsymbol{M}_3^{\mathrm{a}})$ the gravity torque of the asteroid exerted on the MC (SC), $\boldsymbol{M}_2^{\mathrm{c}}$ $(\boldsymbol{M}_3^{\mathrm{c}})$ the control torque exerted on MC (SC), $\boldsymbol{M}_2^{\mathrm{pert}}$ $(\boldsymbol{M}_3^{\mathrm{pert}})$ the perturbation torque of the Sun exerted on the MC (SC).

The gravitational torque of the Sun is determined by the vector pointing from the center of mass of the MC to the Sun and is projected in the frame $o_3x_3y_3z_3$

$${\boldsymbol{M}_2}^{\mathrm{s}} = \frac{3\mu_{\mathrm{s}}}{|\boldsymbol{r}_1 + \boldsymbol{r}_2|^5} \mathbf{A}_2 (\boldsymbol{r}_1 + \boldsymbol{r}_2) \times [\mathbf{I}_2 \mathbf{A}_2 (\boldsymbol{r}_1 + \boldsymbol{r}_2)]. \tag{8}$$

Similarly, the gravitational torque of the asteroid is calculated as

$${\boldsymbol{M}_2}^{\mathrm{a}} = \frac{3\mu_{\mathrm{a}}}{|\boldsymbol{r}_2|^5} \mathbf{A}_2 \boldsymbol{r}_2 \times (\mathbf{I}_2 \mathbf{A}_2 \boldsymbol{r}_2). \tag{9}$$

An offset of ε_2 between the center of pressure and center of mass is assumed to be in the $o_3x_3y_3z_3$ plane and the torque induced by the offset is written in the form

$${\boldsymbol{M}_2}^{\mathrm{solar}} = \begin{bmatrix} 0 & \varepsilon_2 & 0 \end{bmatrix}^{\mathrm{T}} \times {\boldsymbol{f}_2}^{\mathrm{solar}} m_2. \tag{10}$$

The perturbation torque $\boldsymbol{M}_2{}^{\mathrm{pert}}$ is a bounded unknown torque with an upper bound of M_2^{m}

$$\left|\boldsymbol{M}_2{}^{\mathrm{pert}}\right| \leq M_2^{\mathrm{m}}. \tag{11}$$

Besides the gravities of the Sun and asteroid, the solar radiation force exerted on the SC cannot be neglected because of the high intensity of the focused light. The gravities of the MC and other planets are very small and modeled as perturbations. Therefore, the dynamical equations of motion of the SC in the frame $o_3x_3y_3z_3$ can be written as

$$\ddot{\boldsymbol{r}}_3 + 2\boldsymbol{\omega}_2{}^{\mathrm{b}} \times \dot{\boldsymbol{r}}_3 + \boldsymbol{\omega}_2{}^{\mathrm{b}} \times \left(\boldsymbol{\omega}_2{}^{\mathrm{b}} \times \boldsymbol{r}_3\right) + \dot{\boldsymbol{\omega}}_2{}^{\mathrm{b}} \times \boldsymbol{r}_3 = \boldsymbol{f}_3{}^{\mathrm{s}} + \boldsymbol{f}_3{}^{\mathrm{a}} + \boldsymbol{f}_3{}^{\mathrm{solar}} + \boldsymbol{f}_3{}^{\mathrm{c}} + \boldsymbol{f}_3{}^{\mathrm{pert}}, \tag{12}$$

where $\boldsymbol{r}_3$ is position vector from the collector to the reflector in $o_3x_3y_3z_3$.

The acceleration introduced by solar gravitational force is projected in the frame $o_3x_3y_3z_3$ as

$$\boldsymbol{f}_3{}^{\mathrm{s}} = -\frac{\mu_{\mathrm{s}}\left[\boldsymbol{r}_3 + \mathbf{A}_2(\boldsymbol{r}_1 + \boldsymbol{r}_2)\right]}{\left|\boldsymbol{r}_3 + \mathbf{A}_2(\boldsymbol{r}_1 + \boldsymbol{r}_2)\right|^3}. \tag{13}$$

Similarly, the acceleration generated by the gravitational force of the asteroid can be given by

$$\boldsymbol{f}_3{}^{\mathrm{a}} = -\frac{\mu_{\mathrm{a}}\left[\boldsymbol{r}_3 + \mathbf{A}_2\boldsymbol{r}_2\right]}{\left|\boldsymbol{r}_3 + \mathbf{A}_2\boldsymbol{r}_2\right|^3}. \tag{14}$$

The solar radiation acceleration is difficult to model because many uncertainties in the intensity of the solar light exist. If the MC faces the solar light directly and all the light is focused and reflected onto the SC, which will collimate the beam and direct it completely onto the asteroid's surface, the equivalent area of the SC can be regarded as the area of the MC. However, errors may exist in each step of the process of collecting light, and subsequently collimating and reflecting the beam. Instead of modeling the force accurately, this paper focuses on the dynamical and control issues and tries to eliminate the effects of modeling errors by designing the controller. An equivalent area of the second collector, denoted as A, is used to calculated solar radiation pressure forces. Then, the solar radiation pressure acceleration can be written as

$$\boldsymbol{f}_3{}^{\mathrm{solar}} = 2PA(\boldsymbol{n}_3 \cdot \boldsymbol{n}_3{}^{\mathrm{s}})^2\boldsymbol{n}_3/m_3, \tag{15}$$

where P is the solar radiation pressure at the distance of the asteroid; $\boldsymbol{n}_3$ is the normal vector of the SC and $\boldsymbol{n}_3^{\mathrm{s}}$ is along the negative direction of the x_3 axis. The perturbation force $\boldsymbol{f}_3^{\mathrm{pert}}$ is a bounded unknown force with an upper bound of $\boldsymbol{f}_3{}^m$. The relative orientation of the SC with respect to the frame $o_3x_3y_3z_3$ is described by three Euler angles $(\varphi_3, \theta_3, \psi_3)$ of the rotational sequence of $R_3(\psi_3) \leftarrow R_2(\theta_3) \leftarrow R_1(\varphi_3)$ from the frame $o_3x_3y_3z_3$ to the frame $o_rx_ry_rz_r$. The angular velocity components in the frame $o_rx_ry_rz_r$ can be given by

$$\omega_3^{\mathrm{b}} = \begin{bmatrix} \dot{\varphi}_3 - \dot{\psi}_3 S_{\theta_3} \\ \dot{\theta}_3 C_{\varphi_3} + S_{\varphi_3} C_{\theta_3}\dot{\psi}_3 \\ -\dot{\theta}_3 S_{\varphi_3} + \dot{\psi}_3 C_{\varphi_3} C_{\theta_3} \end{bmatrix} + \mathbf{A}_3\left(\boldsymbol{\omega}_2^{\mathrm{b}} + \frac{\boldsymbol{r}_3 \times \dot{\boldsymbol{r}}_3}{\left|\boldsymbol{r}_3\right|^2}\right). \tag{16}$$

where $\boldsymbol{\omega}_3{}^{\mathrm{b}}$ is the angular velocity of the reflector and $\mathbf{A}_3$ is transition matrix frame $o_3x_3y_3z_3$ to $o_{\mathrm{r}}x_{\mathrm{r}}y_{\mathrm{r}}z_{\mathrm{r}}$.

The kinematical differential equations can be solved from Equation (16), given by

$$\dot{\boldsymbol{\chi}}_3 = \begin{bmatrix} \dot{\psi}_3 \\ \dot{\theta}_3 \\ \dot{\varphi}_3 \end{bmatrix} = \begin{bmatrix} \omega_3^y S_{\varphi_3}/C_{\theta_3} + \omega_3^z C_{\varphi_3}/C_{\theta_3} \\ \omega_3^y C_{\varphi_3} - \omega_3^z S_{\varphi_3} \\ -\omega_3^x + \omega_3^y S_{\varphi_3} S_{\theta_3}/C_{\theta_3} + \omega_3^z C_{\varphi_3} S_{\theta_3}/C_{\theta_3} \end{bmatrix} = \boldsymbol{G}_3(\boldsymbol{\omega}_3), \tag{17}$$

where $\chi_3 = (\varphi_3\ \theta_3\ \psi_3)$ are three Euler angles of SC in frame $o_3x_3y_3z_3$, and

$$\boldsymbol{\omega}_3 = \left[\ \omega_3^x\ \ \omega_3^y\ \ \omega_3^z\ \right]^{\mathrm{T}} = \boldsymbol{\omega}_3^{\mathrm{b}} - \mathbf{A}_3\left(\boldsymbol{\omega}_2^{\mathrm{b}} + \frac{\boldsymbol{r}_3 \times \dot{\boldsymbol{r}}_3}{|\boldsymbol{r}_3|^2}\right)$$

The dynamical equations of the attitude in the body-fixed frame can be written as

$$\mathbf{I}_3\dot{\boldsymbol{\omega}}_3{}^{\mathrm{b}} + \boldsymbol{\omega}_3{}^{\mathrm{b}} \times \left(\mathbf{I}_3 \cdot \boldsymbol{\omega}_3{}^{\mathrm{b}}\right) = \boldsymbol{M}_3{}^{\mathrm{s}} + \boldsymbol{M}_3{}^{\mathrm{a}} + \boldsymbol{M}_3{}^{\mathrm{solar}} + \boldsymbol{M}_3{}^{\mathrm{c}} + \boldsymbol{M}_3{}^{\mathrm{pert}}. \tag{18}$$

The gravitational torques of the Sun and the asteroid can be obtained similarly as

$$\boldsymbol{M}_3{}^{\mathrm{s}} = \frac{3\mu_{\mathrm{s}}}{|\boldsymbol{r}_3 + \mathbf{A}_2(\boldsymbol{r}_1 + \boldsymbol{r}_2)|^5}\mathbf{A}_3\left[\boldsymbol{r}_3 + \mathbf{A}_2(\boldsymbol{r}_1 + \boldsymbol{r}_2)\right] \times \left\{\mathbf{I}_3 \cdot \mathbf{A}_3\left[\boldsymbol{r}_3 + \mathbf{A}_2(\boldsymbol{r}_1 + \boldsymbol{r}_2)\right]\right\}, \tag{19}$$

$$\boldsymbol{M}_3{}^{\mathrm{a}} = \frac{3\mu_{\mathrm{a}}}{|\boldsymbol{r}_3 + \mathbf{A}_2\boldsymbol{r}_2|^5}\mathbf{A}_3(\boldsymbol{r}_3 + \mathbf{A}_2\boldsymbol{r}_2) \times \left[\mathbf{I}_3 \cdot \mathbf{A}_3(\boldsymbol{r}_3 + \mathbf{A}_2\boldsymbol{r}_2)\right]. \tag{20}$$

The solar radiation torque is zero when the center of pressure and center of mass coincide with each other. However, there is always an offset in reality. An offset of ε_3 is assumed and the torque induced by the offset can be given by

$$\boldsymbol{M}_3{}^{\mathrm{solar}} = \left[\ 0\ \ \varepsilon_3\ \ 0\ \right]^{\mathrm{T}} \times \boldsymbol{f}_3{}^{\mathrm{solar}} m_3. \tag{21}$$

The perturbation torque M_3^{pert} is a bounded torque with an upper bound of M_3^{m}.

Equations (1), (6), (7), (12), (17) and (18) are the dynamic equations of the whole system, which are nonlinear and coupled with each other. Equations (1) and (7) are the orbit and attitude dynamic equations of the MC. The orbit dynamic equation includes the solar radiation pressure force that is determined by its attitude. The attitude will track the reference attitude generated by the orbit and the reference attitude changes with the vector from the Sun to the asteroid. However, the distance between the asteroid and MC is negligible compared with the distance between the asteroid and the Sun. Therefore, the reference attitude can be regarded as constant in the $o_2x_2y_2z_2$ frame. In addition, the gravitational torques introduced by both the Sun and the asteroid are very small compared with the torque generated by the center of pressure and center of mass offset. The attitude equation of the MC is independent of other equations. For the SC, the solar pressure force is determined by its attitude and the center of mass is designed to track the focal point of the MC. The attitude is designed to track the reference signal that is dependent on the orbit of the two collectors and the attitude of the MC. Therefore, both the orbit and attitude equations are coupled with other equations. To design efficient control methods for the whole system, the equations should be considered simultaneously. The nonlinear sliding-mode control method is employed to design the control method. An important merit of the sliding mode control is that it provides robustness to uncertainties. The control parameters can be selected properly to guarantee that the system with bounded perturbations is asymptotically stable (Jovan et al. 2001).

4 NONLINEAR SLIDING-MODE CONTROL

The MC is desired to be in static equilibrium in the $o_2x_2y_2$ plane. The x_2 coordinate is equal to the focal length of the MC and the y_2 coordinate is determined by the focal length of the SC. The coordinates of static equilibrium are given by

$$\boldsymbol{r}_2{}^r = \left[\ f_1\ \ f_2\ \ 0\ \right]^{\mathrm{T}}. \tag{22}$$

The sliding manifold is chosen to be

$$\boldsymbol{S}_0 = (\boldsymbol{r}_2 - \boldsymbol{r}_2{}^r) + \lambda_0\dot{\boldsymbol{r}}_2, \tag{23}$$

where λ_0 is the weight matrix for the sliding manifold defined by MC orbit.

To guarantee that the system will stay on the sliding manifold when it starts there, the following relation must be satisfied at each instant:

$$\dot{\boldsymbol{S}}_0 = \dot{\boldsymbol{r}}_2 + \lambda_0 \ddot{\boldsymbol{r}}_2 = 0. \tag{24}$$

The aperture of the MC is designed to face the sunlight. The normal vector of the MC that determines the aperture direction can be projected in to the $o_2x_2y_2z_2$ frame as

$$\boldsymbol{n}_2 = {\mathbf{A}_2}^{\mathrm{T}} \left[\begin{array}{ccc} 1 & 0 & 0 \end{array} \right]^{\mathrm{T}}. \tag{25}$$

The reference direction is along the radial direction of the collector, given by

$${\boldsymbol{n}_2}^r = \frac{\boldsymbol{r}_1 + \boldsymbol{r}_2}{|\boldsymbol{r}_1 + \boldsymbol{r}_2|} = \frac{\left[\begin{array}{ccc} r_a + x_2 & y_2 & z_2 \end{array} \right]^{\mathrm{T}}}{|\boldsymbol{r}_1 + \boldsymbol{r}_2|}. \tag{26}$$

The reference Euler angles can be obtained by substituting Equation (26) into Equation (25). The rotation angle along the center axis of the collector can be randomly selected and will not affect the pointing direction of the axis. In our analysis, the rotation angle is defined to be zero. Then, the three reference Euler angles at each instant can be given by

$$\psi_2^r = \tan^{-1} \frac{y_2}{r_a + x_2}, \quad \theta_2^r = -\sin^{-1} \frac{z_2}{|\boldsymbol{r}_1 + \boldsymbol{r}_2|}, \quad \varphi_2^r = 0. \tag{27}$$

The sliding manifold is chosen to be in the following form

$$\boldsymbol{S}_1 = (\boldsymbol{\chi}_2 - {\boldsymbol{\chi}_2}^r) + \lambda_1 (\dot{\boldsymbol{\chi}}_2 - \dot{\boldsymbol{\chi}}_2{}^r), \tag{28}$$

where λ_1 is weight matrix for the sliding manifold defined by the attitude of the MC.

Whenever the system is on the sliding manifold it will stay on it if and only if the following relation is satisfied at each instant:

$$\dot{\boldsymbol{S}}_1 = (\dot{\boldsymbol{\chi}}_2 - \dot{\boldsymbol{\chi}}_2{}^r) + \lambda_1 (\ddot{\boldsymbol{\chi}}_2 - \ddot{\boldsymbol{\chi}}_2{}^r) = 0. \tag{29}$$

The terms of derivatives in the frame $o_2x_2y_2z_2$ can be written as

$$\begin{aligned}
\dot{\boldsymbol{\chi}}_2{}^r &= \left[\begin{array}{ccc} \dot{\psi}_2^r & \dot{\theta}_2^r & \dot{\varphi}_2^r \end{array} \right]^{\mathrm{T}} = \frac{\partial {\boldsymbol{\chi}_2}^r}{\partial \boldsymbol{r}_2} \dot{\boldsymbol{r}}_2, \\
\ddot{\boldsymbol{\chi}}_2{}^r &= \frac{\partial \dot{\boldsymbol{\chi}}_2{}^r}{\partial \boldsymbol{r}_2} \dot{\boldsymbol{r}}_2 + \frac{\partial {\boldsymbol{\chi}_2}^r}{\partial \boldsymbol{r}_2} \ddot{\boldsymbol{r}}_2, \\
\ddot{\boldsymbol{\chi}}_2 &= \frac{\partial \boldsymbol{G}_2}{\partial \boldsymbol{\chi}_2} \boldsymbol{G}_2 + \frac{\partial \boldsymbol{G}_2}{\partial \boldsymbol{\omega}_2} \left(\frac{\partial \boldsymbol{\omega}_2}{\partial \boldsymbol{\chi}_2} \boldsymbol{G}_2 + \frac{\partial \boldsymbol{\omega}_2}{\partial {\boldsymbol{\omega}_2}^{\mathrm{b}}} \dot{\boldsymbol{\omega}}_2{}^{\mathrm{b}} + \frac{\partial \boldsymbol{\omega}_2}{\partial {\boldsymbol{\omega}_2}^{\mathrm{o}}} \dot{\boldsymbol{\omega}}_2{}^{\mathrm{o}} + \frac{\partial \boldsymbol{\omega}_2}{\partial \boldsymbol{r}_2} \dot{\boldsymbol{r}}_2 + \frac{\partial \boldsymbol{\omega}_2}{\partial \dot{\boldsymbol{r}}_2} \ddot{\boldsymbol{r}}_2 \right).
\end{aligned}$$

We want to keep the position of the SC at a constant distance along the central axis of the MC. Therefore, the sliding manifold can be chosen to be a weighted summation of the position error and velocity error

$$\boldsymbol{S}_2 = (\boldsymbol{r}_3 - {\boldsymbol{r}_3}^r) + \lambda_2 \dot{\boldsymbol{r}}_3, \tag{30}$$

where λ_2 is the weight matrix for the sliding manifold defined by the orbit of the SC. To guarantee that the system stays on the sliding manifold, the following relation must be satisfied at each instant:

$$\dot{\boldsymbol{S}}_2 = \dot{\boldsymbol{r}}_3 + \lambda_2 \ddot{\boldsymbol{r}}_3 = 0. \tag{31}$$

The normal is the bisection vector of the incoming and reflected light so that the sunlight after being reflected by the SC will reach the asteroid. The reference direction generated by the orbit of the two collectors can be given by

$$\boldsymbol{n}_{\mathrm{a}} = \frac{1}{2}\left(\frac{\boldsymbol{r}_3}{|\boldsymbol{r}_3|} + \frac{\boldsymbol{r}_3 + \mathbf{A}_2\boldsymbol{r}_2}{|\boldsymbol{r}_3 + \mathbf{A}_2\boldsymbol{r}_2|}\right). \tag{32}$$

The normal of the collector projected in the frame of $o_3x_3y_3z_3$ can be written as

$$\boldsymbol{n}_3 = {\mathbf{A}_3}^{\mathrm{T}}\left[\begin{array}{ccc}1 & 0 & 0\end{array}\right]^{\mathrm{T}}. \tag{33}$$

The reference Euler angles can be calculated similarly as those of the MC. The sliding manifold for the attitude is chosen to be the combination of errors between the instant Euler angles and reference angles

$$\boldsymbol{S}_3 = (\boldsymbol{\chi}_3 - {\boldsymbol{\chi}_3}^r) + \lambda_3\left(\dot{\boldsymbol{\chi}}_3 - {\dot{\boldsymbol{\chi}}_3}^r\right), \tag{34}$$

where λ_3 is the weight matrix for the sliding manifold defined by the attitude of the SC. Here ${\boldsymbol{\chi}_3}^r$ is determined by the vector ${\boldsymbol{n}_3}^r = \frac{\boldsymbol{n}_a}{|\boldsymbol{n}_a|}$. To guarantee that the system stays on the sliding manifold when it starts there, the following relation must be satisfied at each instant:

$$\dot{\boldsymbol{S}}_3 = (\dot{\boldsymbol{\chi}}_3 - {\dot{\boldsymbol{\chi}}_3}^r) + \lambda_3\left(\ddot{\boldsymbol{\chi}}_3 - {\ddot{\boldsymbol{\chi}}_3}^r\right) = 0. \tag{35}$$

The derivatives can be obtained as

$$\begin{aligned}
\dot{\boldsymbol{\chi}}_3 &= \boldsymbol{G}_3, \quad \ddot{\boldsymbol{\chi}}_3 = \frac{\partial \boldsymbol{G}_3}{\partial \boldsymbol{\chi}_3}\dot{\boldsymbol{\chi}}_3 + \frac{\partial \boldsymbol{G}_3}{\partial \boldsymbol{\omega}_3}\left(\frac{\partial \boldsymbol{\omega}_3}{\partial \boldsymbol{\chi}_3}\boldsymbol{G}_3 + \frac{\partial \boldsymbol{\omega}_3}{\partial {\boldsymbol{\omega}_3}^{\mathrm{b}}}{\dot{\boldsymbol{\omega}}_3}^{\mathrm{b}} + \frac{\partial \boldsymbol{\omega}_3}{\partial \boldsymbol{r}_3}\dot{\boldsymbol{r}}_3 + \frac{\partial \boldsymbol{\omega}_3}{\partial \dot{\boldsymbol{r}}_3}\ddot{\boldsymbol{r}}_3\right), \\
{\dot{\boldsymbol{\chi}}_3}^r &= \left[\begin{array}{ccc}\dot{\psi}_3^r & \dot{\theta}_3^r & \dot{\varphi}_3^r\end{array}\right]^{\mathrm{T}} = \frac{\partial \boldsymbol{\chi}_3^r}{\partial \boldsymbol{r}_2}\dot{\boldsymbol{r}}_2 + \frac{\partial \boldsymbol{\chi}_3^r}{\partial \boldsymbol{r}_3}\dot{\boldsymbol{r}}_3 + \frac{\partial \boldsymbol{\chi}_3^r}{\partial \boldsymbol{\chi}_2}\dot{\boldsymbol{\chi}}_2, \\
{\ddot{\boldsymbol{\chi}}_3}^r &= \frac{\partial {\dot{\boldsymbol{\chi}}_3}^r}{\partial \boldsymbol{r}_2}\dot{\boldsymbol{r}}_2 + \frac{\partial \dot{\boldsymbol{\chi}}_3^r}{\partial \boldsymbol{r}_3}\dot{r}_3 + \frac{\partial {\dot{\boldsymbol{\chi}}_3}^r}{\partial \boldsymbol{\chi}_2}\dot{\boldsymbol{\chi}}_2 + \frac{\partial {\boldsymbol{\chi}_3}^r}{\partial \boldsymbol{r}_2}\ddot{\boldsymbol{r}}_2 + \frac{\partial {\boldsymbol{\chi}_3}^r}{\partial \boldsymbol{r}_3}\ddot{\boldsymbol{r}}_3 + \frac{\partial {\boldsymbol{\chi}_3}^r}{\partial \boldsymbol{\chi}_2}\ddot{\boldsymbol{\chi}}_2.
\end{aligned}$$

For the orbit of the MC, a Lyapunov function chosen to satisfy the control method is given by

$$V_0 = \frac{1}{2}{\boldsymbol{S}_{\mathbf{0}}}^{\mathrm{T}}\boldsymbol{S}_{\mathbf{0}}. \tag{36}$$

The derivative of the function can be written as

$$\dot{V}_0 = {\boldsymbol{S}_0}^{\mathrm{T}}\dot{\boldsymbol{S}}_0 = {\boldsymbol{S}_2}^{\mathrm{T}}\left(\boldsymbol{T}_0 + \lambda_0{\boldsymbol{f}_2}^{\mathrm{c}} + {\boldsymbol{f}_2}^{\mathrm{pert}}\right). \tag{37}$$

To guarantee that the derivative is negative, the control force can be implemented as

$$\boldsymbol{T}_0 = \dot{\boldsymbol{r}}_2 + \lambda_0\left[{\boldsymbol{f}_2}^{\mathrm{s}} + {\boldsymbol{f}_2}^{\mathrm{a}} + {\boldsymbol{f}_2}^{\mathrm{solar}} - 2{\boldsymbol{\omega}_2}^{\mathrm{o}} \times \dot{\boldsymbol{r}}_2 - {\boldsymbol{\omega}_2}^{\mathrm{o}} \times ({\boldsymbol{\omega}_2}^{\mathrm{o}} \times \boldsymbol{r}_2) - {\dot{\boldsymbol{\omega}}_2}^{\mathrm{o}} \times \boldsymbol{r}_2\right], \tag{38}$$

For the attitude of the MC, a Lyapunov function chosen to satisfy the control method is given by

$$V_1 = \frac{1}{2}{\boldsymbol{S}_1}^{\mathrm{T}}\boldsymbol{S}_1. \tag{39}$$

The derivative of the function is obtained as

$$\dot{V}_1 = {\boldsymbol{S}_1}^{\mathrm{T}}\dot{\boldsymbol{S}}_1 = {\boldsymbol{S}_1}^{\mathrm{T}}\left(\boldsymbol{T}_1 + \boldsymbol{K}_1{\boldsymbol{M}_2}^{\mathrm{c}} + {\boldsymbol{M}_2}^{\mathrm{pert}}\right). \tag{40}$$

The control torque is taken in the following form:

$$\boldsymbol{M}_2{}^{\mathrm{c}} = {\boldsymbol{K}_1}^{-1}\left[-\boldsymbol{T}_1 - \sigma_1\mathrm{sign}(\boldsymbol{S}_1)\right], \tag{41}$$

where σ_1 is the weight matrix for the sign function, and

$$\begin{aligned}
\boldsymbol{K}_1 &= \lambda_1 \frac{\partial \boldsymbol{G}_2}{\partial \boldsymbol{\omega}_2} \frac{\partial \boldsymbol{\omega}_2}{\partial {\boldsymbol{\omega}_2}^{\mathrm{b}}} {\mathbf{I}_2}^{-1}, \\
\boldsymbol{T}_1 &= \boldsymbol{K}_1 \left[{\boldsymbol{M}_2}^{\mathrm{s}} + {\boldsymbol{M}_2}^{\mathrm{a}} + {\boldsymbol{M}_2}^{\mathrm{solar}} - {\boldsymbol{\omega}_2}^{\mathrm{b}} \times \left(\mathbf{I}_2 \cdot {\boldsymbol{\omega}_2}^{\mathrm{b}} \right) \right] + \boldsymbol{G}_2 - {\dot{\boldsymbol{\chi}}_2}^{r} \\
&+ \lambda_1 \left[\frac{\partial \boldsymbol{G}_2}{\partial \boldsymbol{\chi}_2} \boldsymbol{G}_2 + \frac{\partial \boldsymbol{G}_2}{\partial \boldsymbol{\omega}_2} \left(\frac{\partial \boldsymbol{\omega}_2}{\partial \boldsymbol{\chi}_2} \boldsymbol{G}_2 + \frac{\partial \boldsymbol{\omega}_2}{\partial {\boldsymbol{\omega}_2}^{\mathrm{o}}} {\dot{\boldsymbol{\omega}}_2}^{\mathrm{o}} + \frac{\partial \boldsymbol{\omega}_2}{\partial \boldsymbol{r}_2} \dot{\boldsymbol{r}}_2 + \frac{\partial \boldsymbol{\omega}_2}{\partial \dot{\boldsymbol{r}}_2} \ddot{\boldsymbol{r}}_2 \right) - {\ddot{\boldsymbol{\chi}}_2}^{r} \right].
\end{aligned}$$

To guarantee the asymptotic stability of convergence to the manifold, the derivative of the Lyapunov function should be negative. To guarantee that it has a negative value, the parameter σ_1 should satisfy the condition that each element of σ_1 is larger than M_2^{m}. Similarly, the Lyapunov function for the position control of the SC is chosen as

$$V_2 = \frac{1}{2} {\boldsymbol{S}_2}^{\mathrm{T}} \boldsymbol{S}_2. \tag{42}$$

The derivative of the function can be written as

$$\dot{V}_2 = {\boldsymbol{S}_2}^{\mathrm{T}} \dot{\boldsymbol{S}}_2 = {\boldsymbol{S}_2}^{\mathrm{T}} \left(\boldsymbol{T}_2 + \lambda_2 {\boldsymbol{f}_3}^{\mathrm{c}} + {\boldsymbol{f}_3}^{\mathrm{pert}} \right). \tag{43}$$

To guarantee that the derivative is negative, the control force can be implemented as

$${\boldsymbol{f}_3}^{\mathrm{c}} = -\lambda_2^{-1} \boldsymbol{T}_2 - \lambda_2^{-1} \sigma_2 \mathrm{sign}\left(\boldsymbol{S}_2 \right), \tag{44}$$

where

$$\boldsymbol{T}_2 = \dot{\boldsymbol{r}}_3 + \lambda_2 \left[{\boldsymbol{f}_3}^{\mathrm{s}} + {\boldsymbol{f}_3}^{\mathrm{a}} + {\boldsymbol{f}_3}^{\mathrm{solar}} - 2 {\boldsymbol{\omega}_2}^{\mathrm{b}} \times \dot{\boldsymbol{r}}_3 - {\boldsymbol{\omega}_2}^{\mathrm{b}} \times \left({\boldsymbol{\omega}_2}^{\mathrm{b}} \times \boldsymbol{r}_3 \right) - {\dot{\boldsymbol{\omega}}_2}^{\mathrm{b}} \times \boldsymbol{r}_3 \right].$$

To guarantee that the derivative of the function is negative, the parameter σ_2 should satisfy the condition that each element of σ_2 is larger than ${\boldsymbol{f}_3}^{\mathrm{m}}$. To generate the desired pointing direction of SC, the Lyapunov function is chosen similarly to be

$$V_3 = \frac{1}{2} {\boldsymbol{S}_3}^{\mathrm{T}} \boldsymbol{S}_3. \tag{45}$$

The derivative of the function in the corresponding frame can be given by

$$\dot{V}_3 = {\boldsymbol{S}_3}^{\mathrm{T}} \dot{\boldsymbol{S}}_3 = {\boldsymbol{S}_3}^{\mathrm{T}} \left(\boldsymbol{T}_3 + \boldsymbol{K}_3 {\boldsymbol{M}_3}^{\mathrm{c}} + {\boldsymbol{M}_3}^{\mathrm{pert}} \right). \tag{46}$$

The control law is implemented in the following form to guarantee the asymptotic stability of the system.

$${\boldsymbol{M}_3}^{\mathrm{c}} = {\boldsymbol{K}_3}^{-1} \left[-\boldsymbol{T}_3 - \sigma_3 \mathrm{sign}(\boldsymbol{S}_3) \right], \tag{47}$$

where

$$\begin{aligned}
\boldsymbol{K}_3 &= \lambda_3 \frac{\partial \boldsymbol{G}_3}{\partial \boldsymbol{\omega}_3} \frac{\partial \boldsymbol{\omega}_3}{\partial {\boldsymbol{\omega}_3}^{\mathrm{b}}} {\mathbf{I}_3}^{-1}, \\
\boldsymbol{T}_3 &= \boldsymbol{G}_3 - {\dot{\boldsymbol{\chi}}_3}^{r} + \lambda_3 \left[\frac{\partial \boldsymbol{G}_3}{\partial \boldsymbol{\chi}_3} \boldsymbol{G}_3 + \frac{\partial \boldsymbol{G}_3}{\partial \boldsymbol{\omega}_3} \left(\frac{\partial \boldsymbol{\omega}_3}{\partial \boldsymbol{\chi}_3} \boldsymbol{G}_3 + \frac{\partial \boldsymbol{\omega}_3}{\partial \boldsymbol{r}_3} \dot{\boldsymbol{r}}_3 + \frac{\partial \boldsymbol{\omega}_3}{\partial \dot{\boldsymbol{r}}_3} \ddot{\boldsymbol{r}}_3 \right) \right] \\
&+ \boldsymbol{K}_3 \left[{\boldsymbol{M}_3}^{\mathrm{s}} + {\boldsymbol{M}_3}^{\mathrm{a}} + {\boldsymbol{M}_3}^{\mathrm{solar}} - {\boldsymbol{\omega}_3}^{\mathrm{b}} \times \left(\mathbf{I}_3 \cdot {\boldsymbol{\omega}_3}^{\mathrm{b}} \right) \right].
\end{aligned}$$

To guarantee that the derivative of the function is negative, the parameter σ_3 should satisfy the condition that each element of σ_3 is larger than ${M_3}^{m}$.

Simulation Example: Asteroid Apophis is the object to be deflected and the orbital elements are given in Table 1. Parameters of the MC and SC are presented in Tables 2 and 3.

Table 1 Orbital Elements of the Asteroid

Orbital Elements	a_a (AU)	e_a	i_a (°)	Ω_a (°)	ω_a (°)	f_a (°)
Value	0.92239	0.19104	3.3312	204.462	126.365	0

Table 2 Parameters of the MC

Total Mass (kg)	Propellant (kg)	Radius (m)	$(I_x, I_y, I_z, I_{xy}, I_{xz}, I_{yz})$ (kg m^2)	r_2^r (m)
20 000	5000	315	$(2\times10^6, 1\times10^6, 1\times10^6, 0, 0, 0)$	(2000, –1300, 0)

Table 3 Parameters of the SC

Total Mass (kg)	Propellant (kg)	Radius (m)	$(I_x, I_y, I_z, I_{xy}, I_{xz}, I_{yz})$ (kg m^2)	r_3^r(m) (m)
40	20	20	$(2\times10^3, 1\times10^3, 1\times10^3, 0, 0, 0)$	(–2000, 0, 0)

Table 4 Values of Parameters for Simulation

Parameter	Value
σ_0	1×10^{-8}
σ_1	1×10^{-6}
σ_2	1×10^{-8}
σ_3	1×10^{-6}
λ_0	$(1\times10^5, 1\times10^5, 1\times10^5)$
λ_1	$(1\times10^5, 1\times10^5, 1\times10^5)$
λ_2	$(1\times10^5, 1\times10^5, 1\times10^5)$
λ_3	$(1\times10^4, 1\times10^4, 1\times10^4)$
f_2^m(m s^{-2})	1×10^{-9}
f_3^m(m s^{-2})	1×10^{-9}
M_2^m(Nm)	1×10^{-7}
M_3^m(Nm)	1×10^{-7}
ε_2(m)	0.3
ε_3(m)	0.1

Table 5 Deflection Efficiency Comparisons

SCS	Life Time (d)	89.4
	Velocity Variation (m s^{-1})	0.2128
	Orbital Deflection (km)	2465.2
GT	Life Time (d)	1203.3
	Velocity Variation (m s^{-1})	0.0128
	Orbital Deflection (km)	1109.6
SSGT	Life Time (d)	9627.0
	Velocity Variation (m s^{-1})	0.0869
	Orbital Deflection (km)	60425.7

A total mass of 20 000 kg with 5000 kg of propellant and a radius of 315 m are used for the MC (Melosh et al. 2002). The MC is placed 2000 m away from the SC and the SC is 1300 m above the asteroid, which requires the radius of the SC to be larger than 9.3 m. The radius of the SC is chosen to be 20 m, with a total mass of only 40 kg. The lifetimes of the SC and MC are evaluated to be about

25 min and several years, respectively. Random perturbations with upper bounds are added to the system, and the parameters of the controller are designed based on the values of these upper bounds. The parameters determining the force models and controller are presented in Table 4. The system with small random position and attitude errors is controlled to the desired configuration. The control forces and torques required to initialize and keep the configuration are illustrated in Figure 4. The position and Euler angle errors of the well-controlled system are shown in Figure 5. The propellant with a specific impulse of 3000 s which is required for initialization and station keeping is shown in Figure 6.

5 RESULTS AND DISCUSSION

A lot of simulations have been tested to validate the effectiveness of the controller. The arrangement parameters shown here are just one example. The results show that the controller works well for wide ranges of parameters of the system.

(1) With any initial values in the vicinity of the desired values, the system will converge to the desired values at a speed determined by the parameters of the control law, λ_i ($i = 0, 1, 2, 3, 4$). Larger values achieve faster convergence speed but require larger control forces. The control forces are also dependent on the initial values of the system, and larger initial errors lead to larger control forces with the same parameters of the controller. Therefore, it is suggested that each part of the system be controlled within the vicinity of the desired values by first using optimal energy control values, and then the controller proposed in this paper is employed to keep the system stationary.

(2) The controller can achieve high accuracy with unknown perturbations considered. The position accuracy of the simulation result is about several centimeters and the angular accuracy is about 2×10^{-5} radians. With the distance considered, the position errors induced by the angular errors are also several centimeters.

(3) The forces and torques required for station keeping are used to cancel the solar radiation pressure force and solar radiation torques. For the two collectors, the control forces during the station keeping segment are almost equal to the solar radiation pressure forces and the control torques are almost equal to those generated by the center of pressure and center of mass offset. Therefore, the control torques can be reduced by reducing the offset. However, control forces are always required to cancel the solar radiation pressure forces.

(4) The whole system is similar to the orbiting formation of two collectors in the vicinity of the asteroid. When the system is not controlled to be in the desired configuration, the vaporized mass is very limited and the resultant force exerted on the asteroid is negligible. Therefore, the lifetime of the SC will not be reduced because of the thin mass flow. The initialization has no effect on the deflection and lifetime of the system. In addition, the initialization of the whole system is completed if and only if the initialization of each part is completed. Therefore, the initialization time for each part should be optimized to achieve a compromise. The initialization time of the system is about 6 d and requires less than 6 kg propellant for the SC. The propellant required for station-keeping is very little because the lifetime of the SC is less than one hour. Therefore, the remaining propellant can be used to steer the collector away from the asteroid so that the next collector can be maneuvered into the desired position safely. The propellant of the MC is enough for station keeping for about 2 yr of stationary operations. Therefore, the lifetime of the system is determined by the total lifetime of the SC.

(5) Two design features of a method for asteroid deflection are very important and are always used to judge the feasibility of the method — deflection capability and practicability. The solar collector plan has always been criticized for its impracticability though it possesses the advantage of deflection capability. The most important disadvantages are the physical limitations of the collectors. The first limitation is the requirement of a large solar sail system and the second

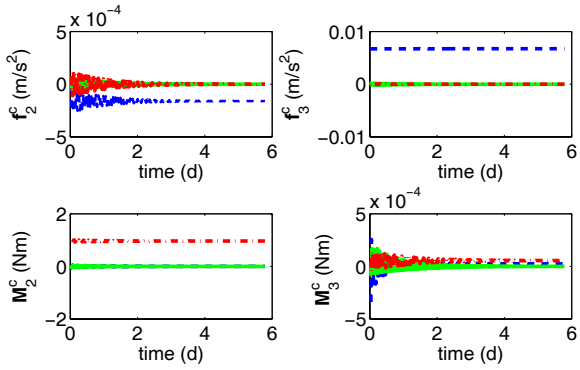

Fig. 4 Control forces for the whole system (*dashed lines*: f_{2x}^c, f_{3x}^c, M_{2x}^c and M_{3x}^c; *solid lines*: f_{2y}^c, f_{3y}^c, M_{2y}^c and M_{3y}^c; *dash-dotted lines*: f_{2z}^c, f_{3z}^c, M_{2z}^c and M_{3z}^c).

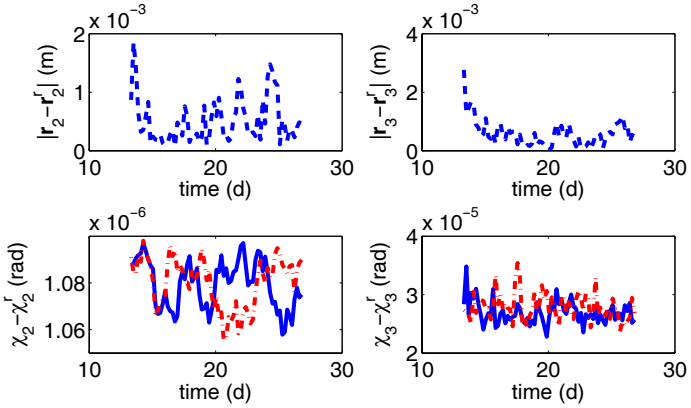

Fig. 5 Position and attitude errors of the controlled system (*solid lines*: $\psi_2 - \psi_2^r$ and $\psi_3 - \psi_3^r$; *dashed lines*: $\theta_2 - \theta_2^r$ and $\theta_3 - \theta_3^r$).

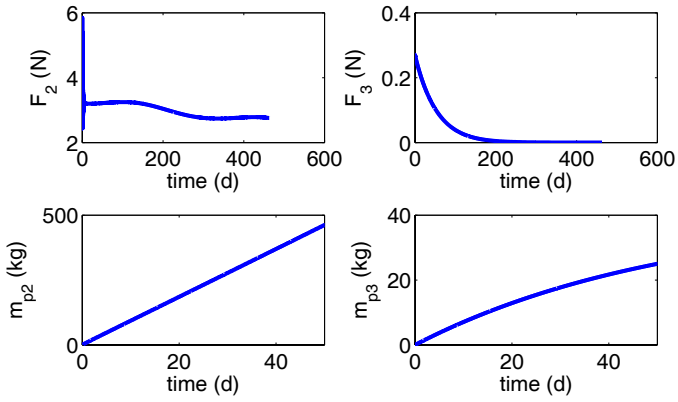

Fig. 6 Control forces and propellant required during station keeping.

one is the short lifetime of the collector immersed in the mass flow. The developments of solar sail technology, including lightweight deployable booms, ultra-lightweight sail films, MEMS and the related deployment technology, would make a large solar sail system possible in the future. Therefore, the short lifetime of the collector becomes a bottleneck for the method. A Cassegrain-like arrangement of two collectors can mitigate the short lifetime effects. As discussed in Melosh et al. (2002), this system requires high-accuracy in the relative position and attitude of the two collectors. In addition, the smaller collector should be abandoned at the end of its life and replaced by a new one. The solar collector is also a non-contact deflection method and similar to a gravitational tractor. The practicability of a deflection method is a systematic and complex problem. It involves many fields. Here, only the deflection capabilities of different methods are compared. The total efficiency of the SCS (Solar Collector System) is assumed to be 0.5 for comparison. The total efficiency may be lower than 0.5 for some design parameters, which does not influence the comparison results. With the conditions given below, the deflection abilities of the SCS, GT (Gravitational Tractor) and SSGT (Solar Sail Gravitational Tractor) are compared.

For the solar collector system, 5000 SCs totally weighing 20 000 kg and an MC weighting 20 000 kg could be launched into space. The next SC would be maneuvered into the desired position at the end of the lifetime of the previous one.

For the GT, two tractors both weighing 20 000 kg, with half the mass being propellant, are placed at static equilibrium points or in a displaced orbit above the asteroid. It is assumed that the thrust is always along the velocity of the asteroid, which means that all the propellant is utilized to deflect the asteroid. The gravitational force of the asteroid generates a constant acceleration of 2×10^{-4} m s^{-2} on the GT, which corresponds to a static equilibrium of about 500 meters above Apophis. The deflection formula in reference (Lu & Love 2005) is employed to calculate the increment of velocity and deflection.

For the SSGT, two tractors both weighing 20 000 kg, with half the mass being propellant, are placed at static equilibrium points above the asteroid. Similarly, the gravitational force of the asteroid generates an acceleration of 2×10^{-4} m s^{-2} on the SSGT and the solar radiation pressure force is used to cancel the gravitation. With the angle between the sunlight and the normal of the solar sail considered; the direction of the solar pressure force cannot be along the velocity of the asteroid (Wie 2007). Therefore, only a component force along the velocity of the asteroid will be used for deflection. A 45° angle between the velocity and the solar pressure force is imposed for the SSGT and the propellant required for station keeping is assumed to be 1/8 of that required by the GT. The deflection formula in reference (Wie 2007) is employed to calculate the increment of the velocity and orbital deflection. In fact, the formation of solar-sail gravity tractors discussed in reference (Gong et al. 2009) can further improve the deflection ability.

The three systems have the same total mass of 40 000 kg and propellant mass of 20 000 kg. According to the simulation results, less than 1000 kg of propellant of the MC is consumed during the lifetime of 5000 SCs. Therefore, the lifetime of the SCS is defined by a summation of the lifetime of all the SCs. The lifetimes of the GT and SSGT systems are determined by the usable propellant. The lifetime of an SC is about 26 min and the lifetime of the whole SCS is about 90 d. There are two important parameters influencing the deflection capability: the induced velocity increments and the time between the deflection operation and the predicted impact on Earth. In the following text, the mission time refers to the time from the operational start time to the predicted impact time. The induced velocity increments and orbital deflections of the three systems during their lifetime are presented in Table 5 and deflection capabilities of the three different systems are illustrated in Figure 7. The SCS is superior to both the GT and SSGT systems and its orbital deflection is about two orders of magnitude higher than those of the two systems for a one-year mission. In addition, the GT generates larger orbit deflections than the SSGT for short missions and the SSGT will demonstrate

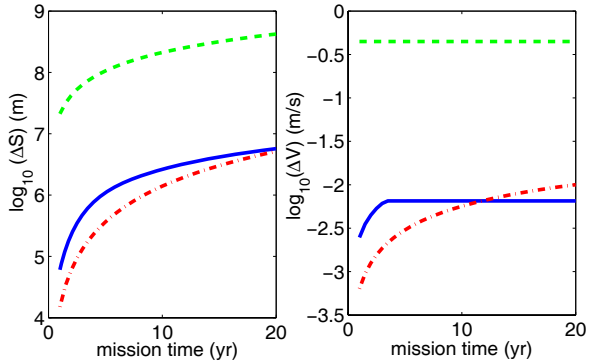

Fig. 7 Deflection and velocity increment of three strategies (*solid lines*: GT, *dash-dotted lines*: SSGT, *dashed lines*: SCS).

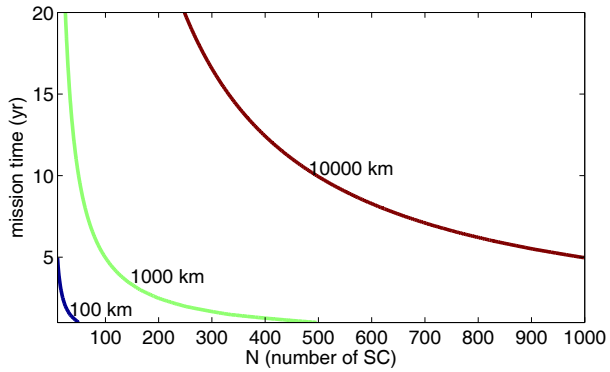

Fig. 8 Capability of the collector system.

its superiority as the mission time increases. The deflection capability of the collector system is illustrated in Figure 8. The number of SCs and mission time required to deflect Apophis a specified distance are presented in the figure. If the operation is applied 20 yr before the predicted impact time, more than 200 SCs are required to deflect Apophis 10 000 km, and a single SC can move the Apophis out of the 600-m keyhole 100 d before the predicted time of impact on Earth.

6 CONCLUSIONS

The dynamics and control aspects of a proposed configuration of a solar collector system is investigated in this paper. One of the drawbacks of the proposed method is the high-accuracy requirements on the relative position and attitude of the MC and SC. The coupled orbit and attitude dynamics of both MC and SC are considered together to design the control method. A sliding-mode control is used to stabilize the system. The simulation results show that high accuracy can be achieved when the unknown perturbations are considered. Finally, the deflection ability of the solar collector system is compared with that of two other deflection strategies. With all the physical limitations considered, the results show that the solar collector generates high efficiency with respect to orbital deflection. If the secondary collector can be re-used after proper handing at the end of its lifetime, the deflection efficiency can be greatly improved.

Acknowledgements This work was funded by the National Natural Science Foundation of China (Grant Nos. 10902056 and 10832004).

Appendix A: LIFETIME CALCULATION

The lifetime of a single collector is evaluated based on the theory in reference (Kahle et al. 2006). The linear arrangement where the ratio of the Sun's diameter to Sun's distance matches the ratio of spot diameter to focal distance of the collector yields

$$d_{\mathrm{spot}} = 2f\frac{R_{\mathrm{sun}}}{r_{\mathrm{NEA}}}. \tag{A.1}$$

The energy balance within the focal point is simplified to be one-dimensional in the perpendicular direction with respect to the asteroid's surface. Lateral heat conduction is neglected because of the small temperature gradient in the given direction. The equation of thermal conduction can be given by

$$\rho c_p \frac{\partial T}{\partial t} = \lambda \frac{\partial^2 T}{\partial x^2}. \tag{A.2}$$

The surface material is assumed to be forsterite and the density is $\rho = 3500\,\mathrm{kg\,m^{-1}}$, the specific heat capacity $c_p = 1000\,\mathrm{J\ kg^{-1}\ K^{-1}}$, and the thermal conductivity $\lambda = 2\,\mathrm{W\ m^{-1}\ K^{-1}}$. These material properties are derived from stone-meterorite data. The heat achieved at the surface is divided into three parts: the first is used for radiation flux; the second is for evaporation and the third for thermal conduction. The energy equilibrium on the surface can be written as

$$q_{\mathrm{spot}} - q_{\mathrm{rad}} - q_{\mathrm{vap}} - \lambda\frac{\partial T}{\partial x} = 0, \tag{A.3}$$

where q_{rad} is the radiation flux and q_{vap} is the heat flux required for evaporation. The radiation flux in an environment of several Kelvin can be approximately given by

$$q_{\mathrm{rad}} = \sigma\varepsilon T_{\mathrm{spot}}^4. \tag{A.4}$$

The energy for evaporation is determined by the enthalpy of the material and the mass flux of evaporation.

$$q_{\mathrm{vap}} = HZ, \tag{A.5}$$

where $H = 8.359\,\mathrm{MJ\ kg^{-1}}$ is the enthalpy of vaporization and Z is the mass flux which can be estimated based on the ideal gas assumption.

$$Z = \frac{p_{\mathrm{spot}}}{\sqrt{2\pi R_s T_{\mathrm{spot}}}}. \tag{A.6}$$

The vapor pressure can be approximated by integrating the Clausius-Clapeyron equation

$$p = C_1 \mathrm{e}^{C_2/T}. \tag{A.7}$$

The constants, $C_1 = 7.62 \times 10^{13}$ Pa and $C_2 = -65.301$ K, are determined by experimental data for forsterite (Nagahara et al. 1992).

From the above primary analysis, we can discover that only 0.05 of the supplied energy is used to vaporize the material. Most of the energy is consumed by radiation and thermal conduction, as shown in Figure A.1.

The vapor outflow is modeled as gas expansion from a reservoir through a nozzle into a vacuum (Komle 1990). The density of the gas in the reservoir is obtained via the ideal gas law

$$\rho_0 = \frac{p_0}{R_s T_0}. \tag{A.8}$$

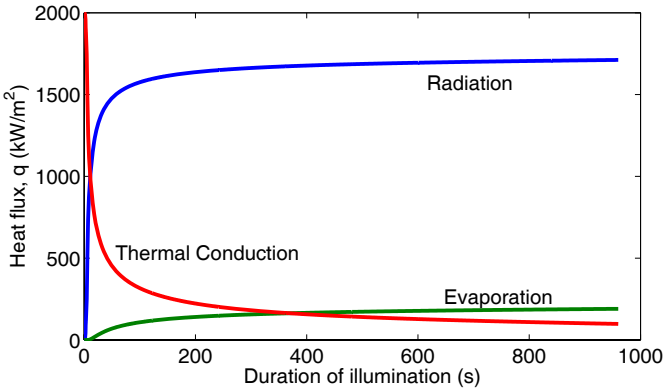

Fig. A.1 Evolution of the heat fluxes for evaporation of forsterite ($q_s = 2MJ\ m^{-2}\ s^{-1}$).

The density of the gas at the nozzle throat is obtained from an isentropic relationship

$$\rho^* = \rho_0 \Big(1 + \frac{\kappa - 1}{2}\Big)^{\frac{-1}{\kappa-1}}, \tag{A.9}$$

where $\kappa = 1.4$ is a constant adiabatic index for diatomic molecules.

Then, the density at an arbitrary distance r and angle θ can be approximated in the continuum flow regime as

$$\rho(r,\theta) = \rho^* A_p \frac{d_{\text{spot}}^2}{(2r + d_{\text{spot}})^2} \left[\cos\left(\frac{\pi\theta}{2\theta_{\text{mas}}}\right)\right]^{\frac{2}{\kappa-1}}. \tag{A.10}$$

The Mach number for the isentropic expansion can be given by

$$\text{Ma}^2 = \frac{2}{\kappa - 1}\Big[\Big(\frac{\rho}{\rho_0}\Big)^{-(\kappa-1)} - 1\Big]. \tag{A.11}$$

The velocity of the gas can be derived from the Mach number as

$$\upsilon = c_0 \text{Ma}\Big(1 + \frac{\kappa - 1}{2}\text{Ma}^2\Big)^{-0.5}, \tag{A.12}$$

where c_0 is sound speed in the reservoir $c_0 = \sqrt{\kappa R_s T_0}$. The temperature and velocity within the free molecular flow regime are treated as constants. The density and pressure are assumed to depend on the distance from the reservoir

$$\frac{p}{p_{Kn=1}} = \frac{\rho}{\rho_{Kn=1}} = \frac{d_{\text{spot}}^2}{4r^2}. \tag{A.13}$$

The gas flow within the freezing zone is simplified to be a sudden transition to free molecular flow. The transition border is defined by $K_n = \frac{l}{L} = 1$, the molecular mean free path $l = \frac{kT}{4\sqrt{2}p\pi r_{\text{mole}}^2}$(Boltzmann constant: $k = 1.3807\times10^{-23}\,\text{J K}^{-1}$; molecular radius: $r_{\text{mole}} = 2\times10^{-10}\,\text{m}$) and the characteristic length is selected to be the focal length $L = f$.

With the above formulas, the pressure and velocity of the gas at any position in space can be calculated. The next step is to evaluate the lifetime of the solar collector when it is placed at different positions.

The grains might impact the sail collector and would decrease the performance. Also, the plume impingement would stick to the surface forming a condensation layer. The growth rate of a layer at an arbitrary point is given by

$$\upsilon_{\text{layer}} = \frac{\upsilon\rho}{\rho_{\text{layer}}}, \tag{A.14}$$

where $\rho_{\text{layer}} = 1\,\text{g cm}^{-3}$ is the layer's density. The height of the layer is $h = \upsilon_{\text{layer}}t$. The fraction of light concentrated by the degraded collector is related to the layer's height, given by

$$\phi = \text{e}^{-2\mu h}, \tag{A.15}$$

where $\mu = 10^4\,\text{cm}^{-1}$ is the absorption coefficient. Therefore, $\phi_s = 0.5$ is used to calculate the lifetime at the position (r, θ)

$$t_{\text{life}} = -\frac{\ln\phi_{\text{s}}}{2\mu}\ \frac{\rho_{\text{layer}}}{\upsilon(r,\theta)\rho(r,\theta)}. \tag{A.16}$$

The solar flux at a distance from the asteroid is labeled S_0. Then, energy concentrated by the MC per unit time can be obtained as $q_{\text{c}} = S_0\pi R_{\text{c}}^2$. The energy flux at the spot of the asteroid is

$$q_{\text{s}} = \eta\frac{S_0\pi R_{\text{c}}^2}{\pi d_{\text{spot}}^2/4} = \eta\frac{4S_0R_{\text{c}}^2}{d_{\text{spot}}^2}$$

with a total efficiency of energy transfer η. The required energy flux on the spot for evaporation is assumed to be q_{s}^0 and Equation (A.1) is combined to generate the following relation

$$f = \frac{r_{\text{NEA}}}{R_{\text{sun}}}\sqrt{\frac{\eta S_0}{q_{\text{s}}^0}}R_{\text{c}}. \tag{A.17}$$

Appendix B: CALCULATION OF THE SOLAR RADIATION PRESSURE FORCE

The infinitesimal area at the position determined by the cone angle γ and clock angle φ can be written as

$$ds = R^2\sin\gamma d\gamma d\varphi. \tag{B.1}$$

The exterior normal at a point can be projected into the body-fixed frame of the collector as

$$\boldsymbol{n}_i = \left[\ \cos\gamma\ \ \sin\gamma\cos\varphi\ \ \sin\gamma\sin\varphi\ \right]^{\text{T}}. \tag{B.2}$$

The projection of the solar light vector in the body-fixed frame is assumed to be $\boldsymbol{n}_{\text{s}}^{\text{b}} = [n_x\ n_y\ n_z]^{\text{T}}$. Then, the solar pressure force of the whole hemisphere can be obtained by integration.

However, some of the interior surface will not be irradiated by the solar light if the solar light offsets the central axis, and the exterior surface of this part is immersed in solar light. The exterior surface will absorb the solar light without reflecting it. This means that the solar radiation pressure force exerted on this part is along the interior normal to each point. Therefore, the resultant solar radiation force exerted on the whole hemisphere is a summation of two parts, labeled $F_i$and F_e: the first part is induced by the solar light pressing the interior surface and the second is exterior to the surface. F_e can be obtained in a local frame with the solar light vector as the y axis and the vector perpendicular to the plane cut by the solar light as the x axis. Then, the force vector can be transformed to the body-fixed frame. The transition matrix can be written as $R_1(-\varphi_{\text{s}})R_3(\pi/2-\gamma_{\text{s}})$

if the solar light vector is rewritten in the form $\boldsymbol{n}_{\rm s}^{\rm b} = \left[\begin{array}{ccc}\cos\gamma_{\rm s} & \sin\gamma_{\rm s}\cos\varphi_{\rm s} & \sin\gamma_{\rm s}\sin\varphi_{\rm s}\end{array}\right]^{\rm T}$. Now, the total solar force exerted on the collector is given by

$$\begin{aligned}\boldsymbol{F}_{\rm s} \;=\; & 2P\int_0^{\pi/2}\int_0^{2\pi}\left(\boldsymbol{n}_i\cdot\boldsymbol{n}_{\rm s}^{\rm b}\right)^2\boldsymbol{n}_i R^2\sin\gamma d\gamma d\varphi \\ & -R_1(-\varphi_{\rm s})R_3(\pi/2-\gamma_{\rm s})3P\int_0^{\gamma_{\rm s}}\int_0^{2\pi}\left(\boldsymbol{n}_i\cdot\boldsymbol{n}_{\rm s}^{\rm b}\right)^2\boldsymbol{n}_i R^2\sin\gamma d\gamma d\varphi, \end{aligned} \tag{B.3}$$

where P is the solar radiation pressure. The solar torque exerted on the mass center of the collector can be similarly calculated. The distance between the center of the sphere and the mass center is $\boldsymbol{L}_0$, so, the vector from the mass center to a point on the surface can obtained as

$$\boldsymbol{L}_i = R\boldsymbol{n}_i - \boldsymbol{L}_0. \tag{B.4}$$

The resultant torque exerted on the collector can be calculated by integration

$$\begin{aligned}\boldsymbol{M}_{\rm s} = {} & 2P\int_0^{\pi/2}\int_0^{2\pi}\left(\boldsymbol{n}_i\cdot\boldsymbol{n}_{\rm s}^{\rm b}\right)^2\left(R\boldsymbol{n}_i-\boldsymbol{L}_0\right)\times\boldsymbol{n}_i R^2\sin\gamma d\gamma d\varphi \\ & -R_1(-\varphi_{\rm s})R_3(\pi/2-\gamma_{\rm s})3P\int_0^{\gamma_{\rm s}}\int_0^{2\pi}\left(\boldsymbol{n}_i\cdot\boldsymbol{n}_s^{b}\right)^2\left(R\boldsymbol{n}_i-\boldsymbol{L}_0\right)\times\boldsymbol{n}_i R^2\sin\gamma d\gamma d\varphi. \end{aligned} \tag{B.5}$$

References

Birch, P. 1992, Journal of the British Interplanetary Society, 45, 331

Early, J. T. 1989, Journal of the British Interplanetary Society, 42, 567

Fogg, M. J. 1995, Warrendale, PA: Society of Automotive Engineers, c1995. 1st ed

Gong, S., Li, J., & Baoyin, H. 2009, Celestial Mechanics and Dynamical Astronomy, 105, 159

Hudson, H. S. 1991, Journal of the British Interplanetary Society, 44, 139

Jovan, D., Li, S. M., & Raman, K. 2001, Journal of Guidance, Control and Dynamics, 24, 14

Kahle, R., Kuhrt, E., Hahn, G., & Knollenberg, J. 2006, Aerospace Science and Technology, 10, 256

Kömle, N. I. 1990, Comet Halley: Investigation, Results, Interpretation 1, Ellis. Horwood, New York

Lu, E. T., & Love, S. G. 2005, Nature, 438, 177

Matloff, G. L. 2008, Acta Astronautica, 62, 334

Maunter, M., & Parks, K. 1990, in Space based climate control, Engineering, Construction, and Operations in Space II, Proceedings of Space 90, ed. Stewart W. Johnson, American Society of Civil Engineers

McInnes, C. R. 2002, Journal of the British Interplanetary Society, 55, 74

McInnes, C. R. 2002, Journal of the British Interplanetary Society, 55, 307

Melosh, H. J., Nemchinov, I. V., & Zetzer, Y. I. 2002, in Hazards Due to Comets and Asteroids, ed. Gehrels T., (Tucson: University of. Arizona Press)

Melosh, H. J. 1993, Nature, 366, 21

Nagahara, H., Kushiro, I., & Mysen, B. O. 1992, Lunar and Planetary Institute Science Conference Abstracts, 23, 959

Oberg, J. E. 1981, New Earths: Restructing Earth and Other Planets (New York: New American Library)

Seifritz, W. 1989, Nature, 340, 603

Wie, B. 2007, in 2007 Planetary Defense Conference, Hovering control of a solar sail gravity tractor spacecraft for asteroid deflection

Zubrin, R. M., & McKay, C. P. 1997, Journal of the British Interplanetary Society, 50, 309